*Inorg. Chem.* **2002**, *41*, 6703–6710

Inorganic Chemistry Article

# Synthesis, Crystal Structures, and Redox Potentials of 2,3,12,13-Tetrasubstituted 5,10,15,20-Tetraphenylporphyrin Zinc(II) Complexes

**Yuichi Terazono, Brian O. Patrick, and David H. Dolphin***

*Department of Chemistry, University of British Columbia, 2036 Main Mall, Vancouver, BC, Canada*

Received May 13, 2002

Zinc(II) complexes of antipodal $\beta$-tetrasubstituted *meso*-tetraphenylporphyrin with trifluoromethyl ($Zn(TPP(CF_3)_4)$ (**1a**)), bromine ($Zn(TPPBr_4)$ (**2a**)), and methyl groups ($Zn(TPP(CH_3)_4)$ (**3a**)) were synthesized in order to examine the steric and the electronic effects of trifluoromethyl groups on the macrocycle. The analysis of X-ray crystal structures of the five-coordinate complexes $Zn(TPP(CF_3)_4)(EtOH)_3$ (**1b**), $Zn(TPPBr_4)(MeOH)(DMF)$ (**2b**), and $Zn(TPP(CH_3)_4)(THF)_{1.6}(CHCl_3)_{0.4}$ (**3b**) revealed distorted macrocyclic cores where significant differences in the Zn–N distance between the $\beta$-substituted and the non-$\beta$-substituted side were observed. The difference was significant in **1b** due to the strong steric interactions among the peripheral substituents and the electronic effects of trifluoromethyl groups. The macrocycles of **1b**–**3b** are saddle-distorted and slightly ruffled due to the five-coordination of zinc(II) and the peripheral substitution. Distortion of the macrocycles of **2b** and **3b** were modest. On the other hand, distortion in **1b** was severe due to the peripheral strain. Cyclic voltammetric measurements of the four-coordinate complexes Zn(TPP) and **1a**–**3a** were performed and their redox potentials were analyzed together with previously reported potentials of $Zn(TPP(CN)_4)$. The oxidation potential of **1a** did not gain as much as expected from the electron-withdrawing effect of the four trifluoromethyl groups. The HOMO–LUMO gap of **1a** was very small (1.5 V) and cannot just be explained by macrocyclic distortion. The magnitude of this gap is very similar to that of $Zn(TPP(CN)_4)$. Compound **2a** also exhibited a modest gap contraction. Compound **3a** was easier to oxidize and harder to reduce than Zn(TPP), even though the HOMO–LUMO gap of **3a** was similar to that of Zn(TPP).

## Introduction

Synthetic porphyrins used in model studies of hemoproteins have been prepared using design strategies involving both structural and electronic modifications. For example, model studies of hemoglobins and myoglobins were driven by sterically hindered synthetic porphyrins into a successful globin-like control of axial ligand coordination.[1−3] Recent examples of structurally modified porphyrins have been involved in studies concerning nonplanarity of the porphyrin macrocycle whose link to the functions of hemoproteins has been suggested.[4−7] Meanwhile, electronically and sterically modified porphyrins, especially incorporating strongly electron-withdrawing substituents, have focused on catalytic oxidations in order to mimic and improve their cytochrome P-450-like activity.[8−10] So far various porphyrins bearing electron-withdrawing substituents such as pentachlorophenyl, pentafluorophenyl, perfluoroalkylphenyl, fluoro, chloro, bromo, cyano, nitro, or perfluoroalkyl groups on *meso* and/or pyrrolic $\beta$-positions of the porphyrin macrocycle have been syn-

* Author to whom correspondence should be addressed. Tel: (604) 822-4571. Fax: (604) 822-9678. E-mail: ddolphin@qltinc.com.

(1) Collman, J. P.; Gagne, R. R.; Halbert, T. R.; Marchon, J. C.; Reed, C. A. *J. Am. Chem. Soc.* **1973**, *95*, 7868.
(2) Almog, J.; Baldwin, J. E.; Huff, J. *J. Am. Chem. Soc.* **1975**, *97*, 227.
(3) Momenteau, M.; Loock, B.; Mispelter, J.; Bisagni, E. *Nouv. J. Chim.* **1979**, *3*, 77.
(4) Barkigia, K. M.; Chantranupong, L.; Smith, K. M.; Fajer, J. *J. Am. Chem. Soc.* **1988**, *110*, 7566.
(5) Nurco, D. J.; Medforth, C. J.; Forsyth, T. P.; Olmstead, M. M.; Smith, K. M. *J. Am. Chem. Soc.* **1996**, *118*, 10918.
(6) Senge, M. O. In *The Porphyrin Handbook*; Kadish, K. M., Smith, K. M., Guilard, R., Eds.; Academic Press: San Diego, 2000; Vol. 1, 239.
(7) Shelnutt, J. A.; Song, X.-Z.; Ma, J.-G.; Jia, S.-L.; Jentzen, W.; Medforth, C. J. *Chem. Soc. Rev.* **1998**, *27*, 31.
(8) Sheldon, R. A. *Metalloporphyrins in Catalytic Oxidations*; Marcel Dekker Inc.: New York, 1994.
(9) Montanari, F.; Casella, L. *Metalloporphyrin Catalyzed Oxidations*; Kluwer Academic Publishers: Dordrecht, 1994.
(10) Dolphin, D.; Traylor, T. G.; Xie, L. Y. *Acc. Chem. Res.* **1997**, *30*, 251 and references therein.

10.1021/ic020339h CCC: $22.00 
Published on Web 11/12/2002

thesized.[11−29] Of the numerous electron-withdrawing groups, perfluoroalkyl groups are unique from a few viewpoints. Perfluoroalkyl groups are inert and strongly $\sigma$-electron-withdrawing, but they do not function as $\pi$-electron donors. Accordingly, perfluoroalkyl groups effectively stabilize the HOMO of the porphyrin macrocycle[30] and provide stable porphyrin ligands. In addition, perfluoroalkyl porphyrins are soluble in a wide range of solvents[27,28] and may be useful as catalysts in special media.[29,31]

Electron-withdrawing and bulky trifluoromethyl groups in $\beta$-trifluoromethyl-*meso*-tetraphenylporphyrins dramatically alter the properties of the macrocycle, compared with those of *meso*-tetraphenylporphyrin.[32] Here, we describe the molecular and electronic properties of the zinc(II) complex of $\beta$-tetrakis(trifluoromethyl)-*meso*-tetraphenylporphyrin examined by X-ray crystal structural analysis and cyclic voltammetric studies. $\beta$-Tetrabromo and $\beta$-tetramethyl derivatives were also synthesized for comparison.

## Experimental Section

**Materials.** All chemicals were purchased from Sigma-Aldrich fine chemicals, Across Chemicals, or Fisher Scientific. Deuterated solvents for NMR measurements were purchased from Cambridge Isotope Laboratories. Chlorinated solvents were filtered using neutral alumina (Fisher, activity I) to remove trace acid. Methylene chloride for cyclic voltammetric measurements was distilled from $CaH_2$, degassed by three cycles of the freeze−thaw pumping, and stored over activated molecular sieves (4 Å). Free-base porphyrins were synthesized as described previously.[32]

**Instrumentation.** UV−visible spectra were recorded on a Varian Cary 50 scan UV−visible spectrophotometer. NMR spectra were recorded on Bruker AC-200 or Avance 300. Cyclic voltammetric measurements were performed with a single-compartment electrochemical cell, a Pine Instrument Co. bipotentiostat model AFCBP1, and Pine Chem sweep voltammetry software for Windows ver. 2.00.

**5,10,15,20-Tetraphenylporphyrinatozinc(II) (Zn(TPP)).** Zn(II) was inserted into $H_2$TPP by a standard procedure.[33] UV−vis ($CH_2Cl_2$): $\lambda_{max}$ (nm) 419, 548, 582. $^1$H NMR ($CDCl_3$): $\delta$ 7.73 (m, 12H, phenyl-*p*- and -*m*-*H*), 8.08 (m, 8H, phenyl-*o*-*H*), 8.90 (s, 8H, pyrr-$\beta$-*H*).

**[2,3,12,13-Tetrakis(trifluoromethyl)-5,10,15,20-tetraphenylporphyrinato]zinc(II) (Zn(TPP($CF_3$)$_4$)) (1a).** $Zn(OAc)_2 \cdot 2H_2O$ (37 mg, 0.17 mmol) in methanol (10 mL) was added to a brown suspension of 7,8,17,18-tetrakis(trifluoromethyl)-5,10,15,20-tetraphenylporphyrin (50 mg, 0.056 mmol) in chloroform (10 mL) at room temperature. The color instantly changed to a bright green, and the solution became homogeneous. The mixture was then stirred for 30 min at room temperature, chloroform (100 mL) was added, and the mixture was washed with water (2 × 100 mL). The volume of the green solution was reduced in vacuo, and the solution was dried over anhydrous sodium sulfate. Filtration and removal of the solvent gave a green powder of the product. The yield was 52 mg (98%). UV−vis ($CH_2Cl_2$): $\lambda_{max}$ (nm) (log $\epsilon$) 442 (5.37), 662 (4.31). $^1$H NMR ($CDCl_3$): $\delta$ 7.70 (m, 12H, phenyl-*m*- and -*p*-*H*), 8.07 (m, 8H, phenyl-*o*-*H*), 8.43 (s, 4H, pyrr-$\beta$-*H*). $^{19}$F NMR ($CDCl_3$): $\delta$ (vs $CFCl_3$) −48.3. CHN anal. (%), calcd for $C_{48}H_{24}F_{12}N_4Zn$: C, 60.68; H, 2.55; N, 5.90. Found: C, 60.60; H, 2.56; N, 5.75.

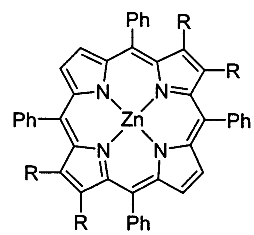


**1a**: R = $CF_3$
**2a**: R = Br
**3a**: R = $CH_3$

**(2,3,12,13-Tetrabromo-5,10,15,20-tetraphenylporphyrinato)zinc(II) (Zn(TPPBr$_4$)) (2a).** Zn(II) was inserted into 7,8,17,18-tetrabromo-5,10,15,20-tetraphenylporphyrin by a standard procedure for the synthesis of metalloporphyrins.[33] LR-MS (EI, 300 °C): $M^+$ (*m*/*z*) = 993; calcd for $C_{44}H_{24}Br_4N_4{}^{64}Zn$, 993.7. UV−vis ($CH_2Cl_2$): $\lambda_{max}$ (nm) 430, 560, 598. $^1$H NMR (DMSO-$d_6$): $\delta$ 8.61 (s, 4H, pyrr-$\beta$-*H*), 8.02 (m, 8H, phenyl-*o*-*H*), 7.80 (m, 12H, phenyl-*p*- and -*m*-*H*). CHN anal. (%), calcd for $C_{44}H_{24}Br_4N_4Zn$: C, 53.18; H, 2.43; N, 5.64. Found: C, 53.25; H, 2.54; N, 5.42.

**(2,3,12,13-Tetramethyl-5,10,15,20-tetraphenylporphyrinato)zinc(II) (Zn(TPP($CH_3$)$_4$) (3a).** The free-base porphyrin (20 mg, 0.030 mmol) was dissolved in chloroform (20 mL). $Zn(OAc)_2 \cdot 2H_2O$ (20 mg, 0.091 mmol) was dissolved in methanol (10 mL) and added to the chloroform solution of the porphyrin. The mixture was refluxed for 1 h. The color of the solution changed from purple to red. After the solvents were removed by rotary evaporation, the product was dissolved in chloroform (60 mL) and washed with water (3 × 60 mL). The solution was dried using anhydrous sodium sulfate. Filtration and evaporation of the solvent yielded a red powder (18 mg, 80%). LR-MS (EI): $M^+$ (*m*/*z*) = 732; calcd for $C_{48}H_{36}N_4{}^{64}Zn$, 732.8. UV−vis ($CH_2Cl_2$): $\lambda_{max}$ (nm) 420, 534sh,


(11) Wijesekera, T.; Matsumoto, A.; Dolphin, D.; Lexa, D. *Angew. Chem., Int. Ed. Engl.* **1990**, *29*, 1028.
(12) Longo, F. R.; Finarelli, M. G.; Kim, J. B. *J. Heterocycl. Chem.* **1969**, *6*, 927.
(13) Woller, E. K.; DiMagno, S. G. *J. Org. Chem.* **1997**, *62*, 1588.
(14) Leroy, J.; Bondon, A.; Toupet, L.; Rolando, C. *Chem. Eur. J.* **1997**, *3*, 1890.
(15) Lyons, J. E.; Ellis, P. E. *Catal. Lett.* **1991**, *8*, 45.
(16) Traylor, T. G.; Tsuchiya, S. *Inorg. Chem.* **1987**, *26*, 1338.
(17) Callot, H. J. *Tetrahedron Lett.* **1973**, 4987.
(18) Callot, H. J. *Bull. Soc. Chim. Fr.* **1974**, 1492.
(19) Duval, H.; Bulach, V.; Fischer, J.; Weiss, R. *Inorg. Chem.* **1999**, *38*, 5495.
(20) Ozette, K.; Leduc, P.; Palacio, M.; Bartoli, J.-F.; Barkigia, K. M.; Fajar, J.; Battioni, P.; Mansuy, D. *J. Am. Chem. Soc.* **1997**, *119*, 6442.
(21) Palacio, M.; Mansuy-Mouries, V.; Loire, G.; Le Barch-Ozette, K.; Ledue, P.; Barkigia, K. M.; Fajar, J.; Battioni, P.; Mansuy, D. *Chem. Commun.* **2000**, 1907.
(22) Ono, N.; Muratani, E.; Fumoto, Y.; Ogawa, T.; Tajima, K. *J. Chem. Soc., Perkin Trans. 1* **1998**, 3819.
(23) Ono, N.; Kawamura, H.; Maruyama, K. *Bull. Chem. Soc. Jpn.* **1989**, *62*, 3386.
(24) Aoyagi, K.; Haga, T.; Toi, H.; Aoyama, Y.; Mizutani, T.; Ogoshi, H. *Bull. Chem. Soc. Jpn.* **1997**, *70*, 937.
(25) Tamiaki, H.; Nagata, Y.; Tsudzuki, S. *Eur. J. Org. Chem.* **1999**, 2471.
(26) Nelson, N. Y.; Medforth, C. J.; Nurco, D. J.; Jia, S.-L.; Shelnutt, J. A.; Smith, K. M. *Chem. Commun.* **1999**, 2071.
(27) Goll, J. G.; Moore, K. T.; Ghosh, A.; Therien, M. J. *J. Am. Chem. Soc.* **1996**, *118*, 8344.
(28) DiMagno, S. G.; Williams, R. A.; Therien, M. J. *J. Org. Chem.* **1994**, *59*, 6943.
(29) Pozzi, G.; Montanari, F.; Quici, S. *Chem. Commun.* **1997**, 69.
(30) Gassman, P. G.; Ghosh, A.; Almlöf, J. *J. Am. Chem. Soc.* **1992**, *114*, 9990.
(31) Horváth, I. T.; Rábai, J. *Science* **1994**, *266*, 72.
(32) Terazono, Y.; Dolphin, D. *J. Org. Chem*., submitted.
(33) Adler, A. D.; Longo, F. R.; Kampas, F.; Kim, J. *J. Inorg. Nucl. Chem.* **1970**, *32*, 2443.

**Table 1.** Crystallographic Data for **1b**−**3b**

| | **1b** | **2b** | **3b** |
|---|---|---|---|
| empirical formula | $C_{54}H_{42}F_{12}N_4O_3Zn$ | $C_{48}H_{35}Br_4N_5O_2Zn$ | $C_{54.80}H_{49.20}N_4ZnO_{1.60}Cl_{1.20}$ |
| fw | 1088.31 | 1098.83 | 897.34 |
| space group | $P\bar{1}$ (No. 2) | $P\bar{1}$ (No. 2) | $P2_1/n$ (No. 14) |
| *a* (Å) | 12.0428(11) | 12.257(2) | 13.585(1) |
| *b* (Å) | 13.275(2) | 13.4377(8) | 18.182(1) |
| *c* (Å) | 16.909(2) | 14.387(1) | 18.065(2) |
| α (deg) | 96.951(5) | 83.819(2) | |
| *β* (deg) | 108.124(2) | 71.227(2) | 93.274(3) |
| *γ* (deg) | 107.354(2) | 73.575(3) | |
| *V* ($Å^3$) | 2383.2(5) | 2151.7(3) | 4454.9(6) |
| *Z* | 2 | 2 | 4 |
| $D_{calc}$ ($g/cm^3$) | 1.52 | 1.70 | 1.34 |
| $\mu$(Mo Kα) ($cm^{-1}$) | 6.13 | 43.42 | 6.70 |
| *T* (°C) | −93 ± 1 | −100 ± 1 | −100 ± 1 |
| no. of indep reflns ($I > 0.00\sigma(I)$) | 10728 | 8177 | 7452 |
| no. of obsd reflns ($I > 3\sigma(I)$) | 5823 | 6086 | 2621 |
| $R^a$ | 0.053 | 0.033 | 0.051 |
| $R_w{}^b$ | 0.091 | 0.089 | 0.155 |

[a] $R1 = \sum||F_o| - |F_c||/\sum|F_o|$, $I > 3\sigma(I)$. [b] $wR2 = [\sum(F_o^2 - F_c^2)^2)/\sum w(F_o^2)^2]^{1/2}$.

551, 587sh. $^1$H NMR ($CDCl_3$): $\delta$ 2.34 (s, 12H, $-CH_3$), 7.75 (m, 12H, phenyl-*m*- and -*p-H*), 8.06 (m, 8H, phenyl-*o-H*), 8.65 (s, 4H, pyrr-*β-H*).

**Zn(TPP(CF$_3$)$_4$)·(EtOH)$_3$ (1b).** Zn(TPP($CF_3$)$_4$ (**1a**) was dissolved in a 50:50 chloroform:ethanol solution, and crystallization of **1b** was induced by slow evaporation at room temperature. After a period of 2 weeks, purple prisms were obtained. $^1$H NMR ($CDCl_3$): $\delta$ 0.34 (t, 3H, EtOH (−O*H*)), 0.73 (t, 9H, EtOH (−C*H*$_3$)), 2.94 (m, 6H, EtOH (−C*H*$_2$−)), 7.70 (m, 12H, phenyl-*m*- and -*p-H*), 8.08 (m, 8H, phenyl-*o-H*), 8.37 (s, 4H, pyrr-*β-H*). $^{19}$F NMR ($CDCl_3$): $\delta$ (vs $CFCl_3$) −48.36. UV−vis ($CH_2Cl_2$) $\lambda_{max}$ (nm) (log $\epsilon$): 444 (5.42), 598sh (3.82), 664 (4.34). CHN anal. (%), calcd for $C_{54}H_{42}F_{12}N_4ZnO_3$: C, 59.60; H, 3.89; N, 5.15. Found: C, 60.00; H, 3.64; N, 5.02.

**Zn(TPPBr$_4$)·(MeOH)·(DMF) (2b).** Crystallization was induced by slow diffusion of methanol into a solution of Zn(TPPBr$_4$) (**2a**) in DMF. After a period of 1−2 days shiny purple chips were obtained. $^1$H NMR could not be measured in $CDCl_3$ because of low solubility. $^1$H NMR (DMSO-$d_6$): $\delta$ 2.75 (s, 3H, DMF (−C*H*$_3$)), 2.89 (s, 3H, DMF (−C*H*$_3$)), 3.22 (d, 3H, MeOH (−C*H*$_3$)), 4.08 (q, 1H, MeOH (−O*H*)), 7.78 (m, 12H, phenyl-*m*- and -*p-H*), 7.99 (s, 1H, DMF (−C*H*O)), 8.02 (m, 8H, phenyl-*o*-H), 8.60 (s, 4H, pyrr-*β-H*). CHN anal. (%), calcd for $C_{48}H_{35}Br_4N_5O_2Zn$ (**2**): C, 52.47; H, 3.21; N, 6.37. Found: 52.32; H, 3.17; N, 6.02.

**Zn(TPP(CH$_3$)$_4$)·(THF)$_{1.6}$·(CHCl$_3$)$_{0.4}$ (3b).** Zn(TPP($CH_3$)$_4$) (**3a**) was dissolved in 50:50 chloroform:tetrahydrofuran, and crystallization was induced by slow evaporation at room temperature. After a period of 1 week, red needle crystals were obtained. $^1$H NMR ($CD_2Cl_2$): $\delta$ 1.76 (m, THF), 2,37 (s, *H*$_2$O), 3.56 (m, THF), 7.25 (s, C*H*Cl$_3$), 7.75 (m, 12H, phenyl-*m*- and -*p-H*), 8.06 (m, 8H, phenyl-*o-H*), 8.65 (s, 4H, pyrr-*β-H*). CHN anal. (%), calcd for $C_{54.8}H_{49.2}Cl_{1.2}N_4O_{1.6}Zn$ (**3**): C, 73.35; H, 5.53; N, 6.24. Found: C, 73.15; H, 5.60; N, 6.06.

**X-ray Crystallography.** All measurements were made on a Rigaku/ADSC CCD area detector with graphite-monochrometed Mo Kα radiation ($\lambda$ = 0.71069 Å). Crystal data and details of the diffraction data collections are given in Table 1. The data were collected at −93 ± 1, −100 ± 1, and −100 ± 1°C to a maximum 2$\theta$ value of 60.2°, 55.7°, and 50.1° at 0.50° oscillations with 80.0, 12.0, and 58.0 s exposures for **1b**−**3b**, respectively. A sweep of data was performed using $\phi$ oscillations from 0.0° to 190.0° at $\chi$ = −90°, −90°, and 0°, and a second sweep was performed using $\omega$ oscillations between −23.0° and 18.0°, −19.0° and 23.0°, and −19.0° and 23° at $\chi$ = −90° for **1b**−**3b**, respectively. The structures were solved by heavy-atom Patterson methods[34] for **1b** and by direct methods[35] for **2b** and **3b** and expanded using Fourier techniques.[36] The non-hydrogen atoms were refined anisotropically. The OH hydrogen atom of the coordinated ethanol was refined isotropically. In **3b**, one disordered molecule of THF coordinated to Zn(II); in addition, two different solvents, THF and $CHCl_3$, partially occupy the same volume in the asymmetric unit. In **3b**, all the disordered solvent molecules were refined isotropically, while all other atoms were refined anisotropically. All calculations were performed using the teXsan crystallographic software package.[37]

## Results and Discussion

**X-ray Crystal Structures.** ORTEP views of the crystal structures for Zn(TPP($CF_3$)$_4$)(EtOH)$_3$ (**1b**), Zn(TPPBr$_4$)(MeOH)(DMF) (**2b**), and Zn(TPP($CH_3$)$_4$)($CHCl_3$)$_{0.4}$(THF)$_{1.6}$ (**3b**) are shown in Figure 1. Selected bond lengths and bond angles for the three molecules together with previously reported data for pentacoordinated Zn(TPP)($H_2O$)[38] are summarized in Table 2.

Coordination around Zn(II) in **1b**−**3b** is pentacoordinate square pyramidal, a common geometry for Zn(II) porphyrins.[39] However, these exhibit the unique core structures commonly observed for antipodal *β*-substituted *meso*-tetraphenylporphyrinato metal complexes such as Ni(TPP(CN)$_4$)(L)$_2$ (L = pyr or 1-meim),[40] (Fe(TPPBr$_4$))$_2$O,[41] Fe(TPPBr$_4$)Cl,[42] or Zn(tTETPP)(pyr);[43] M−N distances are nonequivalent in different N−N vectors (i.e., N1−N3 and N2−N4). The average Zn−N distances for **1b**−**3b** along the N1−N3 vector (i.e., *Zn*−*N* in Table 2) are longer than those along the N2−N4 vector (i.e., Zn−N′ in Table 2). The nonequivalence of the M−N distances is caused by in-plane elongation of the porphyrin core due to the steric strain enforced by the

(34) Beurskens, P. T.; Admiraal, G.; Beurskens, G.; Bosman, W. P.; Garcia-Granda, S.; Gould, R. O.; Smits, J. M. M.; Smykalla, C. PATTY. In *The DIRDIF program system*; Technical Report; Crystallography Laboratory, University of Nijmegen: Nijmegen, The Netherlands, 1992.
(35) Altomare, A.; Burla, M. C.; Cammalli, G.; Cascarano, M.; Giacovazzo, C.; Guagliardi, A.; Moliterni, A. G. G.; Polidori, G.; Spagna, A. *J. Appl. Crystallogr.* **1999**, *32*, 115.
(36) Beurskens, P. T.; Admiraal, G.; Beurskens, G.; Bosman, W. P.; de Gelder, R.; Israel, R.; Smits, J. M. M. *The DIRDIF-94 program system*; Technical Report; Crystallography Laboratory, University of Nijmegen: Nijmegen, The Netherlands, 1994.
(37) *teXsan: Crystal Structure Analysis Package*; Molecular Structure Corp.: The Woodlands, TX, 1985 and 1992.
(38) Golder, A. J.; Povey, D. C. *Acta Crystallogr.* **1990**, *C46*, 1210.
(39) Scheidt, W. R. In *The Porphyrin Handbook*; Kadish, K. M., Smith, K. M., Guilard, R., Eds.; Academic Press: New York, 2000; Vol. 3, 49.
(40) Ni(TPP(CN)$_4$)(L)$_2$: Hexacoordinate (2,3,12,13-tetracyano-5,10,15,20-tetraphenylporphyrinato)nickel(II). L = axial ligand. (a) Reference 19. (b) Duval, H.; Bulach, V.; Fischer, J.; Weiss, R. *Acta Crystallogr.* **1997**, *C53*, 1027.
(41) (Fe(TPPBr$_4$))$_2$O: ($\mu$-Oxo)bis(2,3,12,13-tetrabromo-5,10,15,20-tetraphenylporphyrinato)iron(III). Kadish, K. M.; Autret, M.; Ou, Z.; Tagliatesta, P.; Boschi, T.; Fares, V. *Inorg. Chem.* **1997**, *36*, 204.
(42) Fe(TPPBr$_4$)Cl: Chloro(2,3,12,13-tetrabromo-5,10,15,20-tetraphenylporphyrinato)iron(III). Duval, H.; Bulach, V.; Fischer, J.; Renner, M. W.; Fajer, J.; Weiss, R. *J. Biol. Inorg. Chem.* **1997**, *2*, 662.
(43) Zn(tTETPP)(pyr): Pyridine(2,3,12,13-tetraethyl-5,10,15,20-tetraphenylporphyrinato)zinc(II). Senge, M. O.; Kalisch, W. W. *Inorg. Chem.* **1997**, *36*, 6103.

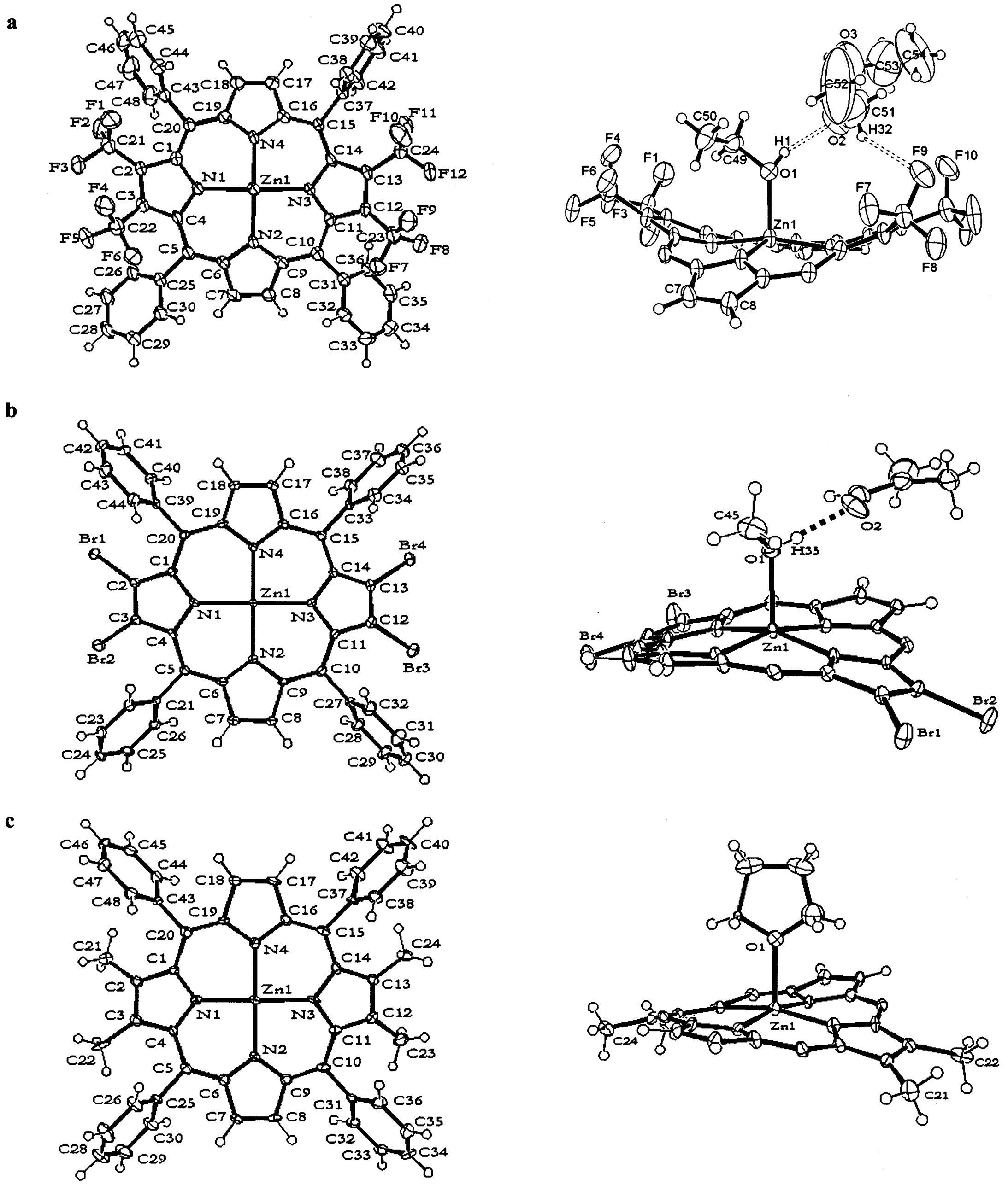


**Figure 1.** X-ray crystal structures of (a) $Zn(TPP(CF_3)_4)(EtOH)_3$ (**1b**), (b) $Zn(TPPBr_4)(MeOH)(DMF)$ (**2b**), and (c) $Zn(TPP(CH_3)_4)(THF)_{1.6}(CHCl_3)_{0.4}$ (**3b**). The axial ligand and the solvated molecules for the top views (left column) and the *meso*-phenyl groups and some solvated molecules for the side views (right column) were omitted for clarity. Ellipsoids are drawn at 30% probability.

peripheral substituents.[39] The mechanism of elongation of the porphyrin core is explained by repulsion of pyrrolic $\beta-\beta$ substituents that push the *meso*-phenyl groups toward the unsubstituted pyrroles. Relief of the peripheral steric strain results in, for example, $C_\beta-C_\beta > C_\beta'-C_\beta'$ and $C_\beta-C_{meso}-C_{ph} > C_\alpha'-C_{meso}-C_{ph}$, as shown in Table 2. This phenomenon is observed for **1b**−**3b**, with **1b** showing the largest elongation. The van der Waals radius of the trifluoromethyl group is estimated to be 2.2 Å[44] (or more),[45] which is larger than that of the methyl (2.0 Å) and the bromine groups (1.95 Å).[46] Thus, of the three Zn(II) porphyrins, the strongest steric interaction among the peripheral substituents is expected in **1b**. As suggested in previous reports,[40,42] the electronic effect of $\beta$-substituents may also contribute to different M−N distances in both vectors; strongly electron-withdrawing substituents on the pyrrolic $\beta$-positions will decrease the electron density on N1 and N3, and the weakened M−N1 and M−N3 bonds will be longer than the other M−N pair. Of the three structures, the difference in the Zn−N distances is largest ($\Delta$Zn−N = 0.117 Å) in **1b** and relatively small ($\Delta$Zn−N = 0.070 Å) in **3b**. While all of the above factors

(44) Smart, B. E. In *Chemistry of Organic Fluorine Compounds II. A Critical Review*; Hudlický, M., Pavlath, A. E., Eds.; American Chemical Society: Washington, DC, 1995.

(45) Kitazume, T.; Yamazaki, T. *Experimental Methods in Organic Fluorine Chemistry*; Kodansha, Gordon and Breach Science Publishers: Tokyo, 1998.

(46) Cotton, F. A.; Wilkinson, G. *Advanced Inorganic Chemistry*, 3rd ed.; Interscience Publishers: New York, 1972.

**Table 2.** Core Size, Selected Bond Lengths (Å), Distances (Å), and Bond Angles (°)

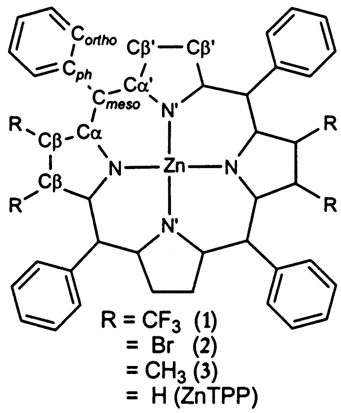


| | **1b** | **2b** | **3b** | Zn(TPP)[a] |
|---|---|---|---|---|
| *N···Ct*[b] | *2.106* | *2.094* | *2.076* | 2.043 |
| N′···Ct | 1.962 | 2.009 | 2.012 | |
| Zn−O | 2.110(3) | 2.108(3) | 2.182(4) | 2.228 |
| *Zn−N* | *2.119(2)* | *2.115(3)* | *2.092(5)* | 2.050 |
| Zn−N′ | 2.002(2) | 2.026(3) | 2.022(5) | |
| *N−$C_\alpha$* | *1.374(3)* | *1.375(4)* | *1.375(7)* | 1.372 |
| N′−$C_\alpha$′ | 1.381(4) | 1.370(4) | 1.377(7) | |
| *$C_\alpha$−$C_\beta$* | *1.451(4)* | *1.448(5)* | *1.456(9)* | 1.442 |
| $C_\alpha$′−$C_\beta$′ | 1.450(4) | 1.446(4) | 1.454(9) | |
| *$C_\beta$−$C_\beta$* | *1.368(4)* | *1.350(5)* | *1.376(9)* | 1.341 |
| $C_\beta$′−$C_\beta$′ | 1.336(4) | 1.344(5) | 1.348(8) | |
| *$C_\alpha$−$C_{meso}$* | *1.422(4)* | *1.409(4)* | *1.419(8)* | 1.405 |
| $C_\alpha$′−$C_{meso}$ | 1.396(4) | 1.401(5) | 1.388(8) | |
| *$C_\alpha$−N−$C_\alpha$* | *108.2(2)* | *108.2(3)* | *105.9(5)* | 106.8 |
| $C_\alpha$′−N−$C_\alpha$′ | 106.6(2) | 106.8(3) | 107.4(5) | |
| *$C_\alpha$−$C_{meso}$−$C_{ph}$* | *118.6(3)* | *119.7(3)* | *118.2(6)* | 117.2 |
| $C_\alpha$′−$C_{meso}$−$C_{ph}$ | 116.0(3) | 115.8(3) | 116.0(5) | |
| $C_\alpha$−$C_\beta$−X1(X4)[c] | 129.0(3) | 129.6(3) | 129.0(6) | |
| $C_\alpha$−$C_\beta$−X2(X3)[c] | 125.0(3) | 129.2(2) | 128.6(6) | |

[a] Reference 38. [b] Ct is the centroid of the four nitrogen atoms. [c] X1 = C21 or Br1, X2 = C22 or Br2, X3 = C23 or Br3, and X4 = C24 or Br4.

contribute to the conformation of **1a**, the major influence on the M−N distances results from the unique 18$\pi$-electron pathway. The free-base $\beta$-tetrakis(trifluoromethyl)-*meso*-tetraphenylporphyrin has a bacteriochlorin-like chromophore where the aromatic system avoids the $CF_3$-substituted carbon atoms.[32] The crystal structure of (2,3,12,13-tetrahydro-5,-10,15,20-tetraphenylporphinato)(pyridine)-zinc(II)[47] shows a similar core distortion with M−N bond lengths of 2.04 and 2.21 Å.

In complexes **1b**−**3b**, the Zn(II) atoms are displaced by 0.325, 0.277, and 0.234 Å from the least-squares plane through the four porphyrin nitrogen atoms (the $N_4$ mean plane). These values are larger than the 0.173 Å for Zn-(TPP)($H_2O$).[38] The value of 0.325 Å for **1b** is especially large compared to those in typical five-coordinate Zn(II) porphyrins with apical Zn−O coordination.[48] Here again two factors, steric and electronic, seem to be affecting the position of the Zn(II) atoms. Displacement of the Zn(II) atoms from the $N_4$ plane occurs due to the larger size of the Zn(II) atom relative to the core sizes of the macrocycles.[39] The core sizes (N···$C_t$ in Table 2) along the N2−N4 vector in **1b**−**3b** are much smaller than that of typical porphyrin ligands like TPP; the largest displacement of the Zn(II) atom in **1b** corresponds to the smallest core size. The Zn−O distances in **1b** and **2b** are about 0.12 Å shorter than the 2.228 Å in Zn(TPP)($H_2O$)[38] or 2.226 Å in Zn(OETPP)(MeOH)[49] but close to that (2.092 Å) in Zn($TPPF_8$)($H_2O$).[14] Presumably, in electron-deficient porphyrins the Zn(II) atoms are pulled out of the porphyrin core by the axial ligand. Thus, the largest Zn(II) atom displacement in **1b** is due to the combination of steric and electronic effects.

Figure 2 shows the magnitude of distortion in the macrocycles of **1b**−**3b**. For all three, pyrrole rings are alternately up and down relative to the $N_4$ mean plane. As shown in the displacements of the pyrrolic α-, $\beta$-, and *meso*-carbons, the pyrrole rings are slightly twisted along the M−N axes. Thus the macrocycles are mainly saddle-distorted and gently ruffled. The average displacements for the pyrrolic $\beta$-carbons from the $N_4$ mean plane for **1b**−**3b** are 0.79, 0.40, and 0.46 Å, respectively. Distortion of the macrocycles of **2b** and **3b** is similar to that in Zn($TPPF_8$)($H_2O$), which is saddle-distorted and has a displacement of 0.49 Å for the pyrrolic $\beta$-carbons.[50] In fact, a potentially planar porphyrin can be distorted by the mode of coordination. For example, crystal structures of a four-coordinate Zn($TPPBr_4$)[51] and a free base of a $\beta$-octafluoro-TPP analogue, $H_2TPPF_{28}$,[52] showed planar porphyrin macrocycles. Thus, the distortion in **2b** and Zn-($TPPF_8$)($H_2O$) seems due to the axial ligand coordination to the Zn(II) atoms. The average displacement of 0.46 Å for pyrrolic $\beta$-carbons from the $N_4$ mean plane in **3b** is more or less the same as that in **2b** and Zn($TPPF_8$)($H_2O$), suggesting that the distortion in **3b** could also be due to the coordination pattern of the Zn(II) atom and that the peripheral steric strain might not be sufficiently large to cause severe macrocyclic distortion. The obviously large average value of 0.79 Å for **1** indicates that factors other than the mode of coordination may be involved in the severe distortion of the macrocycle. Comparison of the root-mean-square values (Figure 2), which are the average deviations of the 24 core atoms from their least-squares plane, also shows the considerable distortion in **1b**. The van der Waals radius of fluorine is close to that of hydrogen.[46] However, the longer C−F bond length (1.3−1.4 Å) compared to the C−H bond length (1.1 Å)[53] makes the $CF_3$ group bulkier than the $CH_3$ group. Thus, steric interactions among the peripheral substituents in **1b** will be larger than those in **3b**. As shown in the top view of **1b** (Figure 1), two *meso*-phenyl groups are extremely twisted due to the steric interaction with trifluoromethyl groups. The average torsion angle made by $C_{ortho}$(C26 or C30)−C25−

(47) Barkigia, K. M.; Miura, M.; Thompson, M. A.; Fajer, J. *Inorg. Chem.* **1991**, *30*, 2233.
(48) Cheng, B.; Scheidt, W. R. *Inorg. Chim. Acta* **1995**, *237*, 5.
(49) Zn(OETPP)(MeOH): Methanol(2,3,7,8,12,13,17,18-octaethyl-5,10,-15,20-tetraphenylporphyrinato)zinc(II). Barkigia, K. M.; Berber, M. D.; Fajar, J.; Medforth, C. J.; Renner, M. W.; Smith, K. M. *J. Am. Chem. Soc.* **1990**, *112*, 8851.
(50) Zn($TPPF_8$)($H_2O$): Aqua(2,3,7,8,12,13,17,18-octafluoro-5,10,15,20-tetraphenylporphyrinato)zinc(II). The value is the displacement from the porphyrin least-squares plane. Reference 14.
(51) Zou, J.-Z.; Li, M.; Xu, Z.; You, X.-Z. *Jiegou Huaxue* **1997**, *16*, 29.
(52) $H_2TPPF_{28}$: 2,3,7,8,12,13,17,18-Octafluoro-5,10,15,20-tetrakis(pentafluorophenyl)porphyrin. Leroy, J.; Bondon, A.; Toupet, L. *Acta Crystallogr.* **1999**, *C55*, 464.
(53) *Handbook of Chemistry & Physics*, 81st ed.; CRC Press: Boca Raton, FL, 2000−2001; p 9-5.

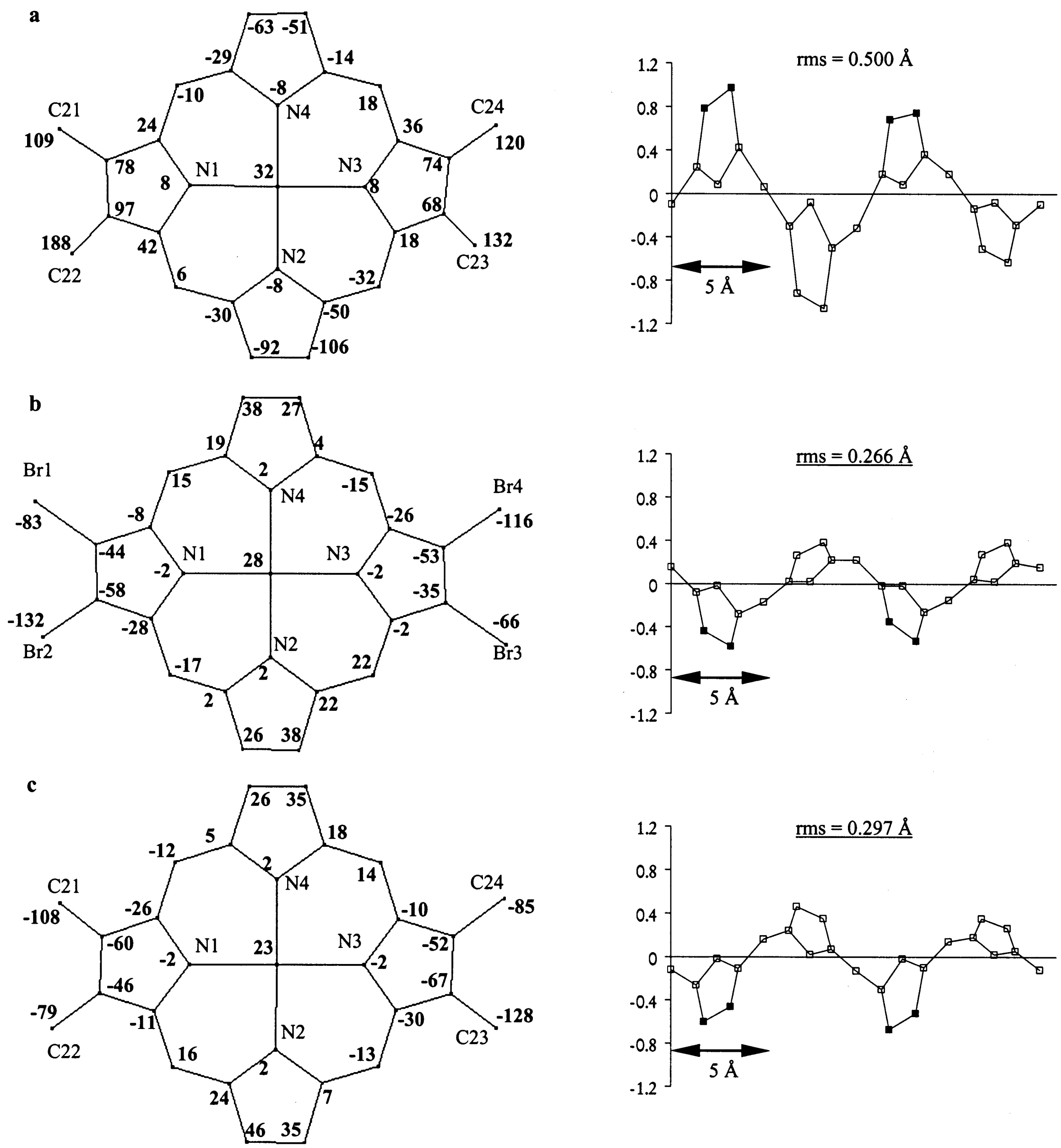


**Figure 2.** Displacements (in 0.01 Å units) of the porphyrin core, pyrrolic $\beta$-substituents, and Zn(II) atom relative to the $N_4$ mean plane (left column) and linear display (in Å units) of the skeletal deviations from the $N_4$ mean plane (right column) of (a) $Zn(TPP(CF_3)_4)(EtOH)_3$ (**1b**), (b) $Zn(TPPBr_4)(MeOH)$-(DMF) (**2b**), and (c) $Zn(TPP(CH_3)_4(THF)_{1.6})(CHCl_3)_{0.4}$ (**3b**). ■ indicates the pyrrolic carbons bearing substituents. The rms values show the average deviation of the 24 core atoms from their least-squares plane.

C5−$C_\alpha$(C4 or C6) is 54.4°, and similarly 52.1° for the other phenyl ring (C31−36). Interestingly, two other phenyl rings (C37−42 and C43−48) are almost orthogonal to the best plane of the porphyrin macrocycle (the corresponding torsion angles are 85.2° and 80.2°, respectively). The crystal structure of **1b** viewed from a different angle (Figure 3) shows that the twisting angles of phenyl rings C25−30 and C31−36 affect those of phenyl rings C37−42 and C43−48. The steric interaction between phenyl ring C43−48 and trifluoromethyl group CF1−3 determines the orientation of the trifluoromethyl group so that no fluorine of F1−3 is pointing at the face of the phenyl ring. This orientation forces F3 to point at the adjacent CF4−6, which orients so that F3 points between F4 and F5. The orientation of CF4−6 is such that the phenyl ring C25−30 cannot lie orthogonal to the porphyrinato core due to the penetration of F6 into the $\pi$-cloud of ring C25−30. In order to avoid this situation, the phenyl ring rotates to reduce the contact with CF4−6. The relatively small $C_\alpha$−$C_\beta$−X2 angle for **1b** (Table 2) indicates that phenyl ring C25−30 is pushed away by CF4−6. Thus, an electrostatic repulsion between the $\pi$-cloud of the phenyl rings and the trifluoromethyl groups appears to be the major driving force for the macrocyclic distortion. Such interactions between fluorine atoms and the $\pi$-electrons of phenyl rings have been reported.[54] It should be noted that the 282 MHz $^{19}F$ NMR spectrum of **1b** in $CDCl_3$ at room temperature displayed a sharp singlet at −48.4 ppm (vs $CFCl_3$), and this equivalency of the trifluoromethyl fluorines indicates rotation of the groups in solution.

The average torsion angles made by the $C_{ortho}$−$C_{Ph}$−

(54) Hayashi, N.; Mori, T.; Matsumoto, K. *Chem. Commun.* **1998**, 1905.

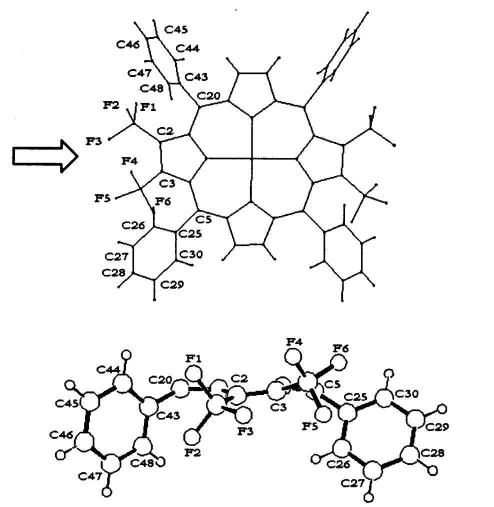

**Figure 3.** Orientations of *meso*-phenyl and $\beta$-trifluoromethyl groups in $Zn(TPP(CF_3)_4)(EtOH)_3$ (**1b**).

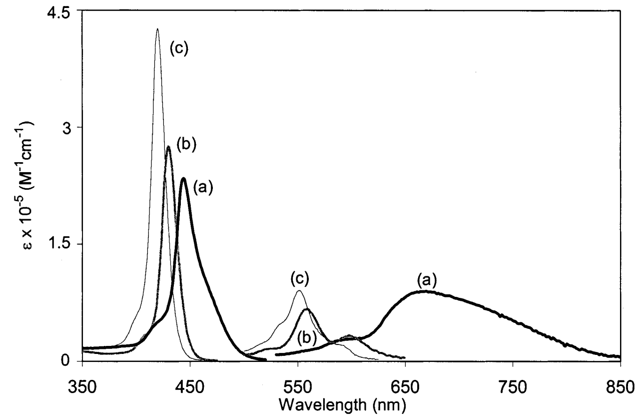


**Figure 4.** Optical spectra of (a) **1a**, (b) **2a**, and (c) **3a** in $CH_2Cl_2$. Q-bands are magnified by five times.

$C_{meso}-C_{\alpha}$ are 68.4°, 78.2°, 76.8°, and 72.9° in **2b** and 75.9°, 67.6°, 71.5°, and 71.3° in **3b**, such that no severe interaction of the phenyl and pyrrolic $\beta$-substituents was observed.

Another interesting feature of the crystal structure of **1b** is coordination of the axial ligand and the macrocycle distortion. Buckling of the macrocycles along the N1−N3 vector (i.e., $\beta$-substituted direction) for **1b** is different from that for **2b** and **3b**. In square-pyramidal coordination of five-coordinate metalloporphyrins, the metal atom is displaced from the $N_4$ mean plane toward the axial ligand and this displacement is accompanied by doming of the porphyrinate core.[55] In the case of **1b**, doming of the porphyrinate core seems to be hampered by the severe steric interaction among the peripheral substituents.

As shown in Figure 1, the axial ethanol is hydrogen bonded to the second ethanol (O2···H1 (1.90 Å)), whose methylene hydrogen (H32) has a nonbonding contact with F9 (F9···H32 (2.71 Å)). The third ethanol is also hydrogen-bonded to the second ethanol (O3···H31 (2.03 Å), where O3 is the oxygen atom in the third ethanol and H31 is the hydroxyl hydrogen of the second ethanol). This network of hydrogen bonding is no doubt enhanced by the extreme electron deficiency of the zinc indued by the peripheral trifluoromethyl groups. There were also some other F···H nonbonding contacts within 3 Å between solvent ethanols, $\beta$-pyrrolic hydrogen, or phenyl ring hydrogen and trifluoromethyl moieties across the different porphyrin units. Intermolecular $^{\delta+}C-F^{\delta-}$ and $^{\delta-}C-H^{\delta+}$ bond dipole interactions or C−H···F−C hydrogen bonding is well-known.[44] Nonbonding contacts between ethanol molecules and trifluoromethyl groups in solution are also suggested by the high-field shifts of the ethanol peaks ($\delta$ 0.34 (t, −O*H*); 0.73 (t, −C*H*$_3$); 2.94 (m, −$CH_2$−)) in the $^1H$ NMR spectrum of **1b** in $CDCl_3$. The large high-field shifts of the ethanol signals of **1b**, compared to free ethanol in $CDCl_3$ ($\delta$ 1.18 (t, −C*H*$_3$); 2.05 (bs, −O*H*); 3.65 (q, −C*H*$_2$−)), indicates that the ethanol molecules in **1b** exist in the pocket created by the four trifluoromethyl groups where they are shielded by the ring current of the macrocycle. It is not possible that the intramolecular hydrogen bonding in **1b**, shown in Figure 1, is the rationale for the mode of buckling, since we also observed similar coordination and distortion patterns for a crystal structure of $Co^{II}(TPP(CF_3)_4)$(pyr),[56] which has no such bonding.

**Optical Spectra.** Figure 4 shows the optical spectra of **1a**−**3a**. **3a** shows a spectrum similar to that of Zn(TPP) (419, 548, and 582 nm), while **2a** shows a small red shift. Compound **1a**, on the other hand, exhibits a unique optical spectrum. The extremely red-shifted Q-band is indicative of a narrower HOMO−LUMO, see below, which is caused by both the macrocyclic distortion[4] and the bacteriochlorin-like electronic structure.[32] It is interesting to note that [*meso*-tetrakis(trifluoromethyl)porphyrinato]zinc(II) ($\lambda_{max}$, nm (log $\epsilon$) 409 (5.27), 554 (3.99), 593 (4.29)),[27] where the four $CF_3$ groups are bonded to the *meso* positions, exhibits an optical spectrum[27] similar to that of Zn(TPP).

**Redox Potentials of Zn(II) Porphyrins.** In the previous section, the relationship between the optical properties and structures was described briefly. In addition, we have also attempted to analyze the electronic structures of the Zn(II) porphyrins using cyclic voltammetry. Cyclic voltammetric measurements were performed using the four-coordinate complexes $Zn(TPP(CF_3)_4)$ (**1a**), $Zn(TPPBr_4)$ (**2a**), and $Zn(TPP(CH_3)_4)$ (**3a**). As presented in Figure 5a, two reversible one-electron waves were observed for **1a**. The first oxidation and reduction potentials of **1a** ($\beta$-$CF_3$), **2a** ($\beta$-Br), **3a** ($\beta$-$CH_3$), Zn(TPP) ($\beta$-H), and $Zn(TPP(CN)_4)$[57] ($\beta$-CN) are plotted against the $4\sigma_p$ value (Figure 5b).[58] As the $4\sigma_p$ value increases, both the oxidation (removal of an electron from the HOMO) and reduction (filling of an electron into the LUMO) potentials increase. The first oxidation potentials change almost linearly. A slight deviation of the first

(55) Scheidt, W. R. In *The Porphyrins*; Dolphin, D., Ed.; Academic Press: New York, 1978; p 463.

(56) $Co(TPP(CF_3)_4)$(py): Pyridine[2,3,12,13-tetrakis(trifluoromethyl)-5,10,15,20-tetraphenylporphyrinato]cobalt(II). Manuscript in preparation.

(57) $Zn(TPP(CN)_4)$: (2,3,12,13-Tetracyano-5,10,15,20-tetraphenylporphyrinato)zinc(II). Source for the redox potentials of $Zn(TPP(CN)_4)$: Giraudeau, A.; Callot, H. J.; Gross, M. *Inorg. Chem.* **1979**, *18*, 201.

(58) $\sigma_p$ values for the substituents were obtained from ref 58a. See ref 58b for the redox potentials vs $\sigma$ values. (a) Hansch, C.; Leo, A.; Taft, R. W. *Chem. Rev.* **1991**, *91*, 165. (b) Kadish, K. M.; Morrison, M. M. *J. Am. Chem. Soc.* **1976**, *98*, 3326.

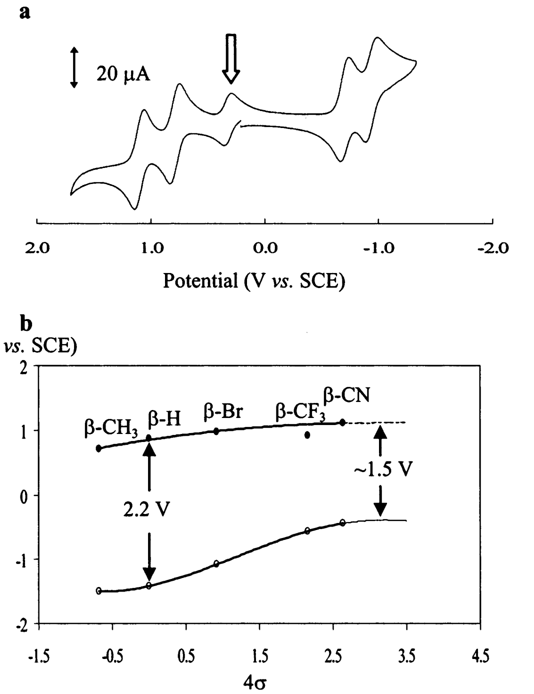


**Figure 5.** Cyclic voltammetric analysis of the four-coordinate antipodal $\beta$-tetrasubstituted *meso*-tetraphenylporphyrin Zn(II) complexes: (a) cyclic voltammogram of **1a** in $CH_2Cl_2$ at [**1a**] = 0.001 M, [$TBAPF_6$] = 0.1 M, and a scan rate of 50 mV/s, and (b) $4\sigma_p$ vs the first oxidation (●) and the first reduction (○) potentials. The white arrow in part a of the figure indicates the internal reference; ferrocene/ferrocenium coupling.

oxidation potential for **1a** ($\beta$-$CF_3$) from this curve is about 0.2 V, which is probably off set by the porphyrin macrocycle distortion. Previous studies have shown that oxidation of the macrocycle is sensitive to structural changes of the porphyrin and the reduction is not; nonplanarity of the macrocycle contributes to lowering the energy level of the HOMO, and that of the LUMO changes linearly with the electron-withdrawing effect of the substituents regardless of the structural changes of the macrocycle.[59−61] The plots of the reduction potentials in Figure 5b show an interesting result, in which the reduction potential is not proportional to the sum of the $\sigma_p$ value, and the plots show a gentle sigmoid curve. The number of available data is limited, but the plots show that both oxidation and reduction potentials seem to be leveling off at higher $4\sigma_p$ values leading to a narrow HOMO−LUMO gap. It is unlikely that the four-coordinate Zn(II) complexes except for **1a** have very distorted macrocycles, and crystal structure analysis for hexacoordinate Ni(II) complexes of $\beta$-tetracyano-TPP showed coplanarity of the porphyrinato ligand. This implies that macrocyclic distortion is also unlikely in the four-coordinate Zn(TPP(CN)$_4$). Thus, the HOMO−LUMO gap contraction should be mainly related to the electronic effect of the $\beta$-substituents. In a recent report, we demonstrated that a dramatic HOMO−LUMO gap contraction is observed for the free bases of $\beta$-trifluoromethyl-*meso*-tetraphenylporphyrins with a fixed 18$\pi$-electron pathway.[32] Thus, the large HOMO−LUMO gap contraction in **1a** presumably originates from its unique electronic structure. In $\beta$-octasubstituted porphyrins the electronic effect of peripheral substituents does not normally affect the HOMO−LUMO gap whereas macrocyclic distortion does.[59] It should be noted that the gap contraction observed for the antipodally $\beta$-substituted electron-deficient porphyrins such as **1a** or Zn(TPP(CN)$_4$) is significantly larger (>600 mV) when compared to an offset by severe macrocyclic distortion (<500 mV for Zn(II) complexes of $\beta$-octabromoporphyrins[61,62]). It also should be noted that the HOMO−LUMO gap of [*meso*-tetrakis(trifluoromethyl)porphyrinato]zinc(II) (Zn(P($CF_3$)$_4$))[27] has been reported as 2.15 V (in benzonitrile), which is similar to that of Zn(TPP). The large difference between **1a** and Zn(P($CF_3$)$_4$) indicates that the position of the groups affects the HOMO−LUMO gap greatly. The electronic effect of the groups in **3a** is not significant.

## Conclusion

A comparative analysis of the structures of three 2,3,12,13-tetrasubstituted porphyrins determined by X-ray crystallography revealed that the electronic and steric effects of pyrrolic $\beta$-trifluoromethyl groups on the macrocycle are dramatic. Steric interactions between the trifluoromethyl and phenyl groups and the strong electron-withdrawing effect of the trifluoromethyl groups are the driving force for the severe macrocycle in-plane and out-of-plane distortions. The electronic structure, specifically of **1a**, also reveals the dramatic effects of the $\beta$-trifluoromethyl substitution where, as with the free base,[32] the 18$\pi$-aromatic system is locked and avoids the atoms bearing these groups.

**Acknowledgment.** We thank Prof. Brian James and his group in the Department of Chemistry at the University of British Columbia for their generous support of the cyclic voltammetric measurements. This work was supported by the Natural Science and Engineering Research Council of Canada.

**Supporting Information Available:** Table of redox potentials of **1a**−**3a**. X-ray crystallographic files in CIF format. This material is available free of charge via the Internet at http://pubs.acs.org.

IC020339H

(59) Takeuchi, T.; Gray, H. B.; Goddard, W. A., III. *J. Am. Chem. Soc.* **1994**, *116*, 9730.
(60) Ochsenbein, P.; Ayougou, K.; Mandon, D.; Fischer, J.; Weiss, R.; Austin, R. N.; Jayaraj, K.; Gold, A.; Terner, J.; Fajar, J. *Angew. Chem., Int. Ed. Engl.* **1994**, *33*, 348.
(61) D'Souza, F.; Zandler, M. E.; Tagliatesta, P.; Ou, Z.; Shao, J.; Van Caemelbecke, E.; Kadish, K. M. *Inorg. Chem.* **1998**, *37*, 4567.
(62) Hodge, J. A.; Hill, M. G.; Gray, H. B. *Inorg. Chem.* **1995**, *34*, 809.